Diachronic and historical evolution of the Al-Hoceima Bay coastline, Moroccan Mediterranean Sea

Mustapha Lamgharbaj[1] ✉ iD, Issam Etebaai*[1] ✉ iD, Morad Taher[1] ✉ iD,
Soukaina Ed-Dakiri[1] ✉ iD, Said El Moussaoui[1] ✉ iD, Hajar El Talibi[1] ✉ iD,
Benyounes Abdellaoui[2] ✉ iD, Hinde Cherkaoui Dekkaki[1] ✉ iD

[1] Abdelmalek Essaadi University, Faculty of Science and Technique,
Team of Applied Geosciences and Geological Engineering, Av. 9 Avril, 2117, Tetouan, Morocco

[2] National Institute of Fisheries Research, Oceanographic and Ecosystem Modeling Laboratory,
Dradeb, PO box 5268, 90000, Tangier, Morocco

* Corresponding author

Abstract: Al-Hoceima Bay, located on the northern coast of Morocco, holds significant environmental importance. It also faces environmental challenges, including the pressures resulting from urban sprawl and growing number of tourists, as well as the impacts of climate change. The objective of this study is to assess the coastal changes in Al-Hoceima Bay since 1964, considering both natural and human factors. This study is based on the diachronic analysis of aerial photographs taken over a period of 56 years, utilising the digital shoreline analysis system statistical technique to calculate the shoreline's mobility index for each period. The results demonstrate significant erosion at the Tayth beach (-1.50 m·y^{-1}) and Souani beach (approximately -1.90 m·y^{-1}), whereas accretion was experienced at the Sfiha beach at a rate of about $+1.11$ m·y^{-1} and at the Lharch beach at a rate of $+0.92$ m·y^{-1}. The mouth of the Nekôr River experienced the highest retreat at -3.15 m·y^{-1}, followed by Ghiss at -2.00 m·y^{-1}. These findings indicate the impact of human interventions, such as the construction of the Mohamed Ben Abdelkarim El Khattabi dam on Oued Nekôr since 1981, as well as climate changes that have led to decreased flow, particularly at Oued Ghiss. These combined climatic and anthropogenic impacts have exacerbated erosion and disrupted the sediment balance along the shoreline of Al-Hoceima Bay.

Keywords: climate change, digital shoreline analysis system, erosion, rate of change, shoreline

INTRODUCTION

Coastal areas, known for their valuable ecosystem services and remarkable ecological and biological productivity (Barbier *et al.*, 2011; Himes-Cornell, Grose and Pendleton, 2018), are favoured by humans when constructing tourist facilities and infrastructure (Hakkou *et al.*, 2018; Benkhattab *et al.*, 2020). Currently, more than 44–60% of the world's population lives within 150 km of the coast (Syvitski *et al.*, 2005; Boye *et al.*, 2018). According to Bird

(1985), a shoreline refers to the boundary where land and a body of water meet. In addition, as stated by Bird (1985), coastal erosion affects more than 70% of the world's beaches.

Shorelines are subject to progressing and rapid changes because of various natural and human-related factors, leading to a very dynamic situation (Jayakumar and Malarvannan, 2016; Muskananfola, Supriharyono and Febrianto, 2020). Climatic conditions, tectonic activity, hydrodynamic forces, and geomorphic processes influence natural factors. These factors include

storm surges, sea-level rise, winds, tidal movements, and land subsidence, and erosion and deposition processes (Hossain *et al.*, 2022). However, anthropogenic factors mainly stem from human activities, and the construction of ports and the growth in the tourist sector are the main contributors. These anthropogenic interventions can alter the natural balance of coastal areas and affect coastal stability (Mageswaran *et al.*, 2021; Santos *et al.*, 2021).

Coastal areas face significant challenges related to the mobility and alteration of coastlines (Chen *et al.*, 2019; Santos *et al.*, 2021). These issues are complex and have far-reaching implications. In recent years, shoreline position has emerged as one of the prominent environmental concerns affecting coastal zones globally (Sheik and Chandrasekar, 2011; Luijendijk *et al.*, 2018). Approximately 70% of the world's coastlines experience erosion, with rates varying from 1 cm·y^{-1} to 10 m·y^{-1} (Luijendijk *et al.*, 2018). On a global scale, erosion affects more than 72% of sandy coasts, and 24% of the beaches have been eroded at rates exceeding 0.5 m per year. In addition, 28% of the beaches have been accreted, and 48% have remained stable in the last three decades (Luijendijk *et al.*, 2018). In Africa, coastal erosion is aggravated by the construction of ports and protective structures in the area of the Mediterranean Sea and Atlantic Ocean. These human interventions play a crucial role in the degradation of the coastal environment in the region (Aouiche *et al.*, 2016).

Morocco has a coastline of more than 3500 km on two Atlantic and Mediterranean fronts, and these coastal areas are not free from erosion. As a result, several studies have been conducted on the Atlantic front, which shows a retreat of the coastline, particularly in the bay of Agadir (Aouiche *et al.*, 2016), the coasts of Agadir and Taghazout (Aangri *et al.*, 2022), the Kenitra coast (Moussaid *et al.*, 2015), and the Tahaddart coast (El Habti *et al.*, 2022). Similarly, on the Mediterranean coast of Morocco, several studies carried out point to coastal degradation in several locations (El Mrini *et al.*, 2012; Benkhattab *et al.*, 2020; Salim *et al.*, 2021). In addition, many research projects have focused on the degradation of coastal areas worldwide, including the Sidi Abdel Rahman coast area in Egypt (Badr Hussein, Ibrahim and Mousa, 2023) and the coast of Chile (Martínez *et al.*, 2022).

The coastal fringe of Al-Hoceima Bay is part of the Moroccan Mediterranean coast. Stretching along more than 40 km of coastline, it is limited to the east by Cape Quelates (Rass Terf), to the west by Cap El Abed, and in the centre by the Ghiss–Nekôr plain. The coastal area has experienced significant influence linked to the socioeconomic development of the region, including urban expansion, as well as the construction of industrial and tourist facilities. The objective of this paper is to quantify the rate of coastal change along Al-Hoceima Bay since 1964 and to identify the main factors contributing to the transformation of the morphology of the coastal environment in the study area. This study draws on the interpretation of four aerial photographs spanning 56 years, divided into four periods: 1964–2003, 2003–2010, 2010–2020, and 1964–2020. This segmentation allows to characterise coastal dynamics over time. To quantify the rate of coastal change, the digital shoreline analysis system (DSAS) method was used, specifically employing the end point rate (*EPR*) technique.

MATERIALS AND METHODS

STUDY AREA

The site of this study is the coastline of Al-Hoceima Bay, which spans approximately 40 km along the central Rif coastline (Taher *et al.*, 2022). It is situated on the northern coast of Mediterranean Morocco, between latitude 35°15'16" N and 35°17'0" N and longitude 3°40'54" W and 3°56'38" W (Fig. 1). The study area is limited by two capes, Quelates to the east and Maure to the west, with the Alboran Sea to the north and the Ghiss–Nekôr plain to the south. The coastline of Al-Hoceima Bay is characterised by the presence of two types of coasts: a soft coast that develops in the central part of the bay (the Ghiss–Nekôr plain) and a rocky coast in the western and eastern parts (Capes Maure and Quelates). The soft central part, consisting of sandy beaches, stretches from the Sfiha beach to the east of the Lharch beach over a distance of about 12 km (Fig. 1), with some small, steep beaches along the rocky coasts. This central part is defined by the presence of the main water sources that nourish this coastline, namely, the rivers of Ghiss and Nekôr. The two capes, Maure and Quelates, are characterised by rocky and cliffy coasts in the western and eastern parts, with varying steep to medium slopes. The western coast extends from Cape Maure to the western extremities of the Sfiha beach, covering a distance of approximately 7 km. This coast is characterised by the presence of small beaches interspersed along its length.

The bay of Al-Hoceima has three major geological formations. The first formation is the central part of the Ghiss–Nekôr plain, which is largely open. It is composed of alluvial deposits dating from the Pliocene to the Quaternary periods. These deposits mainly consist of pebbles, conglomerates, and sand (Nouayti *et al.*, 2022). The second formation in the eastern part of this bay is characterised by the presence of volcanic rocks from the Miocene to the Pliocene periods (Achalhi *et al.*, 2016; Boubkari *et al.*, 2022). Lastly, the western part of the bay is characterised by the Bakkoya limestone ridge (Benaissa *et al.*, 2024). The hydrodynamics in these areas are primarily influenced by frequent swells coming from the W–NW direction. These swells have a short fetch and have a relatively low impact on accretion compared with those originating from the NE to E–NE sector. The swells from the NE to E–NE sector, with their longer fetch, are the primary factors to be considered (Lamgharbaj *et al.*, 2021). The energy of the swells from the NE sector induces a coastal drift from E to W (Lamgharbaj *et al.*, 2021).

MATERIALS

The data used to determine the rate of shoreline evolution consist of aerial photographs taken in 1964, 2003, 2010, and 2020, covering a period of 56 years. The aerial photographs from 1964 and 2010 were acquired from the National Institute, whereas the images from 2003 and 2020 were downloaded from Google Earth (Tab. 1). These aerial photos were taken during an agitated period, and the study area is characterised by a microtidal regime. The shoreline changes in Al-Hoceima Bay over 56 years (1964–2020) was analysed using statistical techniques in the digital shoreline analysis system (DSAS). This approach to data processing involves several steps: (1) aerial photographs were geometrically corrected using known landmarks as control points and imagery referencing
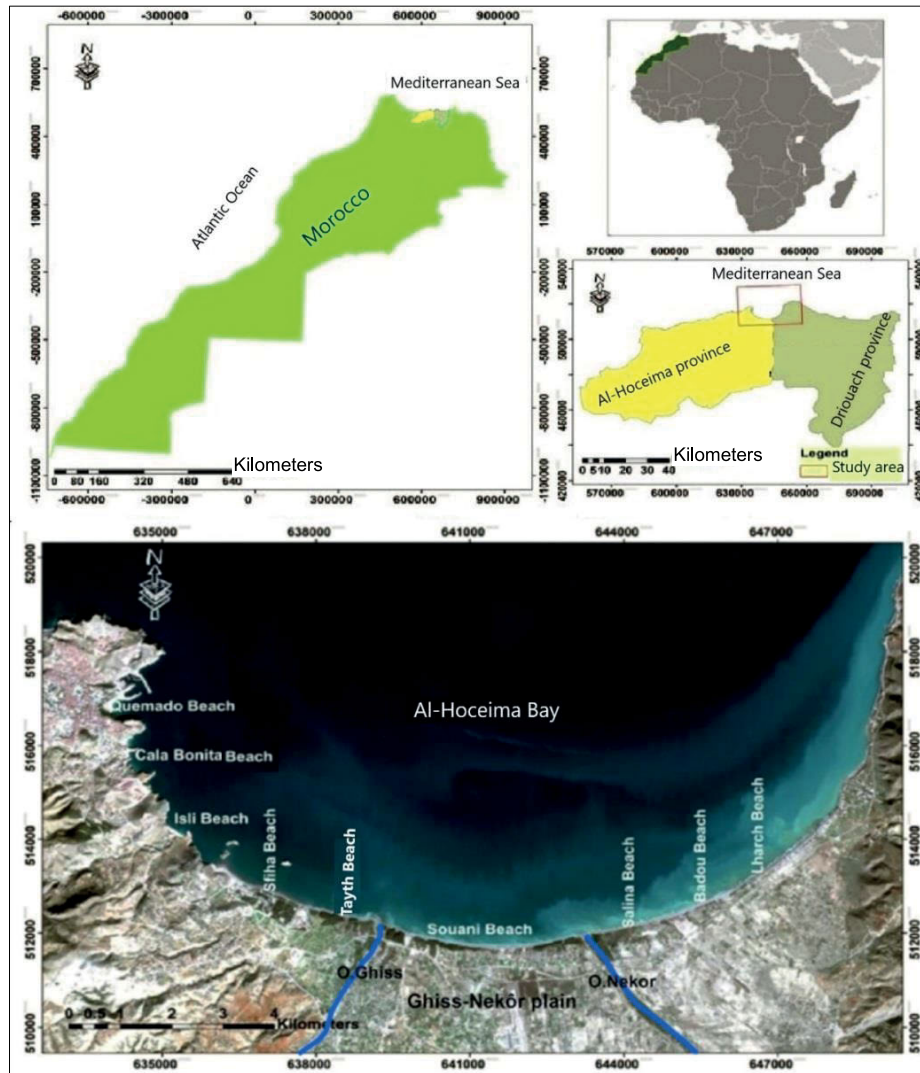
Fig. 1. Location of the study area – Al-Hoceima Bay, Morocco; source: own elaboration

Table 1. Input data used to analyse the shoreline change in Al-Hoceima

Date	Mission reference	Scale of aerial photographs	Pixel size (m)	No. of photographs used	Image type
7 July 1964	ING	1/20,000	1	4	black and white
5 August 2003	Google Earth	–	0.90	3	colour
5 February 2010	ING	1/20,000	2	9	colour
6 August 2020	Google Earth	–	0.90	3	colour

Source: own elaboration.

using the ENVI tool, (2) the shoreline was digitized using GIS software (ArcGIS 10.8), and (3) the rate of shoreline evolution for each period was calculated using the DSAS application.

STUDY METHODS

Image processing

In this study, the methods are based on superposition and interpretation of multi-date imagery. High-resolution ortho-graphic images (1:10,000 and 1:20,000 scales) were used to quantify the rate of change in coastal areas along the coast of Al-

Hoceima Bay. Images for each date were scanned at 600 dpi (42 mm). Photos were not taken vertically from an altitude, which makes it impossible to take measurements on these oblique photographs. Therefore, a sequence of geometric corrections was applied to each image to obtain a presentation between the locations of the photos and those of the environment area (Shin and Kim, 2015). Georeferencing for each image was carried by the ENVI tool. This georeferencing in ENVI relies on control points selected for their stability and visibility, such as road intersections, building corners, and ground markers, which are evenly distributed across each image. These points are used to accurately align

the target image with the reference image through a polynomial transformation. An additional geometric correction is then applied to minimise residual distortions. This method of geo-referencing involves using multiple control points and reference images to ensure accuracy. In addition, geometric correction was used from image to image, and the system of projection used Lambert Conformal Conic Zone 1 Datum Merchich.

Reference line choice

The selection or definition of a coastline reference line is a major problem (Crowell, Leatherman and Buckley, 1991; Boak and Turner, 2005). The high-water line is one of the criteria used to digitise the shoreline (Fenster and Dolan, 1994). This area is identified as the wave boundary (Lanfelder, Stafford and Amein, 1970). During field trips, this reference line is easily distinguish-able due to visible with changes in sand colour, which are marked by beach flooding at high tide (Pajak and Leatherman, 2002). In this study, the high-water line for the soft or sandy coasts was chosen to determine the rate of change in the coastal environ-ments of Al-Hoceima Bay.

The images from each date were accurately georeferenced. The coastline digitisation was performed using ArcGIS. The DSAS 4.2 application, integrated into ArcGIS, was employed to determine the rate of change for each period. The DSAS 4.2, developed by the U.S. Geological Survey, enables the measure-ment of a distance between two shorelines and generates statistics in meters per year by creating transects perpendicular to a defined baseline, calculating the endpoint rate (*EPR*) of shoreline movement, and providing detailed statistical analysis of coastal changes over time.

Baseline data

The rate of change was calculated using the DSAS model version 4.3. DSAS is an application developed by the U.S. Geological Survey that operates under ArcGIS software (Thieler *et al.*, 2009). This tool is used to compile statistics for a series of coastlines. Before using this tool, a geodatabase was created, which included a shoreline for each date and an imaginary line called the baseline for each specific period. Using the DSAS tool, various analyses and calculations were performed (Kumar Das *et al.*, 2021). The rate of change was determined by measuring the distance to the intersection from two points. Finally, the DSAS tool helped to generate a statistical table based on the selected mobility index. The DSAS method involves three steps to develop statistics for each period: (1) merging two shorelines; (2) creating the baseline, which is an imaginary line positioned in the sea or on land; and (3) calculating a statistical index provided by the DSAS tool. In addition, transects with a spacing of 80 m and a length of 400 m were generated perpendicular to the baseline (Fig. 2).

Endpoint rate (*EPR*)

The *EPR* is a coastal mobility index that is calculated using the DSAS tool. It is primarily used to determine the rate of change between two shorelines from different dates. The *EPR* is calculated by measuring the distance difference between the older and the more recent shorelines. This method involves checking the *EPR* index in the DSAS tool and downloading the corresponding statistics. It enables the measurement of the gap between the two lines. The *EPR* index is expressed in meters per year by Equation (1):
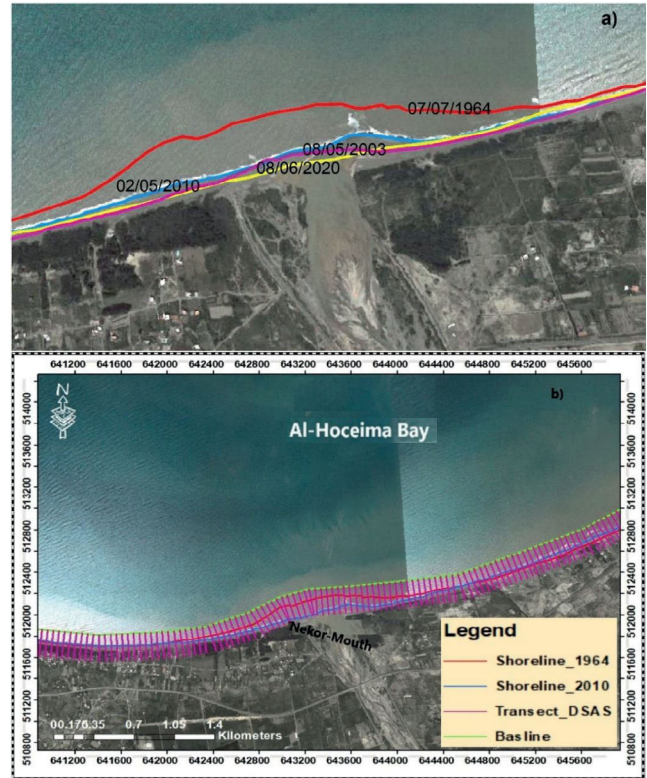

Fig. 2. Clip from an aerial image representing: a) the position of the coastline in different years (1964, 2003, 2010, and 2020), b) an output from shoreline analysis system in ArcGIS, showing shoreline positions and transects generated along the coast; source: own elaboration

$$EPR = \frac{d2 - d1}{t2 - t1} \qquad (1)$$

where: $d2 - d1$ = distance between the two shorelines in meters, $t2 - t1$ = period between the two dates in years.

Error estimation and uncertainty

Various sources of error impact the accuracy of shoreline positions and the rates of shoreline change. This study considers two main categories of uncertainty: positional uncertainty and measurement uncertainty (El Habti *et al.*, 2022). The measure-ment errors associated with shoreline, methods have been estimated in multiple studies (Ford, 2011; Carruthers *et al.*, 2023). Examining coastal evolution through photo interpretation is subject to four types of errors: error during digitisation (E_d), pixel error (E_p), rectification error (E_r), and fluctuations in the position of the high-water line caused by high tide-level variations (E_{td}). Equation (2) expresses the total error (E_t) in shoreline position (Fletcher *et al.*, 2012). The (E_t) considers all measure-ment errors by taking the square root of the sum of the squares. A separate (E_t) was calculated for each period and each shoreline (Tab. 2). The annual error (E_a) of each period (t) was determined according to Equation (3) (Fletcher *et al.*, 2012):

$$E_T = \pm\sqrt{(E_{dt})^2 + (E_p)^2 + (E_r)^2 + (E_d)^2} \qquad (2)$$

$$E_a = \frac{\pm\sqrt{(E_{dt})^2 + (E_p)^2 + (E_r)^2 + (E_d)^2}}{t} \qquad (3)$$

Table 2. Uncertainties and estimated errors, with the shoreline position in metres

Parameter	Uncertainty source			
	1964	2003	2010	2020
Pixel error (E_p)	1.18	1.00	1.18	1.00
Tidal fluctuation error (E_{td})	±0.45	±0.55	±0.50	±0.60
Digitisation error (E_d)	±4.00	±4.00	±2.00	±4.00
Rectification error (E_r)	±0.64	±0.56	±0.40	±0.40
Total error (E_t) (m·y⁻¹)	±4.24	±4.19	±2.40	±4.19
Error of point rate calculation (m·y⁻¹)	±0.15 (1964–2003)	±0.68 (2003–2010)		±0.48 (2010–2020)

Source: own elaboration.

RESULTS

RATE CHANGES FROM 1964 TO 2003

While analysing the results, a minus sign was used to indicate the rate of erosion and a plus sign was used to represent the rate of accretion in the coastal segment under examination. Furthermore, the obtained rate of change was analysed for each period. For spatial analysis of erosion and accretion rates, two specific areas were examined: (1) the central coastline plain and (2) the western area of Al-Hoceima Bay, with a focus on long-term changes in the central plain.

Analysis of the results focused on changes in the shoreline of Al-Hoceima Bay from 1964 to 2003 (Fig. 3). Most statistics were calculated using the DSAS model and the *EPR* mobility index. In general, the shoreline during this period was characterised by predominant erosion along the shore, particularly in the coastal

areas of the Ghiss–Nekôr plain (transects 13–115). The rate of erosion was observed at two river mouths, namely Ghiss and Nekôr, as well as at the beaches of Tayth and Souani. The maximum rate of erosion was localised at the Nekôr mouth, reaching approximately −2.60 m·y⁻¹ (Tab. 3). The retreat of the coastline can be attributed to multiple factors. The first factor is the construction of the Mohamed Ben Abdelkarim El Khattabi (MBK) dam on the Oued Nekôr, which began in 1981. The dam construction has likely altered the natural sediment supply to the coastline, leading to erosion. The second factor is climate change, which has resulted in noticeable changes in recent decades. These changes have led to a decrease in river flow, particularly in the case of Ghiss (Nouayti *et al.*, 2022). During this period, the Al-Hoceima region experienced three pronounced drought periods in 1980–1984, 1994–1995, and 1998–2000 (El-Khantoury, Obda and Achiban, 2020). Drought has the potential to affect the natural evolution and balance of the Al-Hoceima Bay coastline because of a reduction in the quantity of debris carried by the two rivers. Reduced river flow can affect sediment deposition along the coastline, contributing to erosion. However, accretion of the coastline during this period was observed at two beaches, namely, Sfiha and Lharch. Accretion refers to the process of sediment deposition, resulting in expansion or stability of the shoreline. The maximum rate of erosion observed at the mouth of Nekôr is approximately −3.07 m·y⁻¹ (transect 120). Shoreline retreat was observed along the coast of the Ghiss–Nekôr plain. Conversely, the maximum rate of accretion was observed at the Lharch beach, with a rate of approximately +0.79 m·y⁻¹. Accretion of coastline at the Lharch beach can be attributed to the action of coastal drift and the accumulation of sediment.

RATE CHANGE FROM 2003 TO 2010

The period 2003–2010 was marked by significant change in the coastal morphology of the Ghiss–Nekôr plain (Fig. 4). Analysis of statistics by the DSAS numerical model, based on the *EPR*
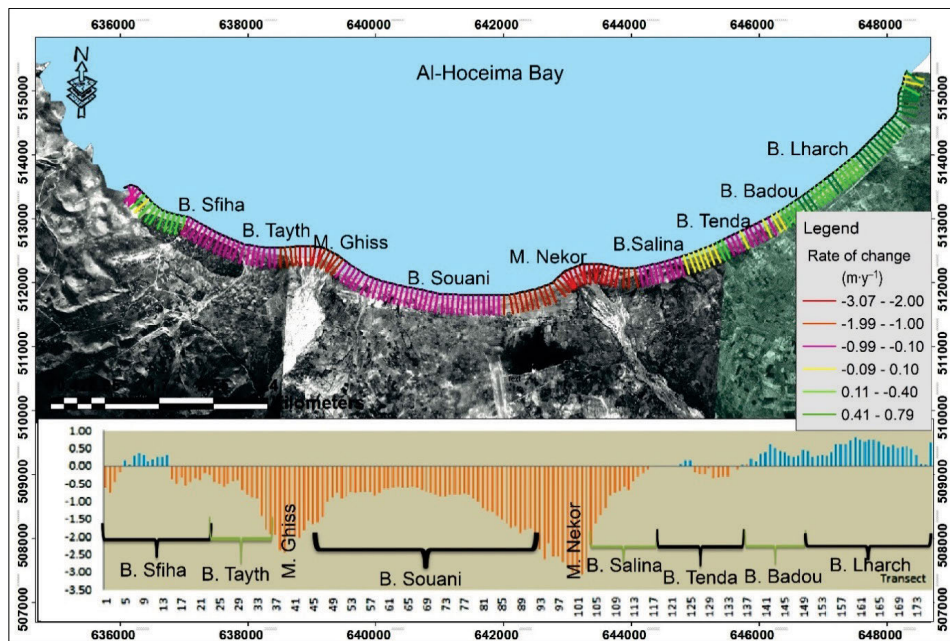
Fig. 3. Shoreline evolution between 1964 and 2003 carried out by the end point rate (*EPR*) statistical method along the coastline of Al-Hoceima Bay; B. = beach, M. = mouth; source: own study

Table 3. Assessment of beaches erosion and accretion in Al Hoceima Bay (1964–2003) using *EPR* index

Specification	Beach							
	Sfiha		Tayth	Souani	Salina	Tenda	Badou	Lharch
Transect No.	8	25	33	91	108	136	143	167
$EPR^{1)}$ (m·y^{-1})	+0.44	−0.99	−1.49	−1.49	−1.49	−0.56	+0.69	+0.79
Evolution evaluation	accretion	erosion	erosion	erosion	erosion	erosion	accretion	accretion

[1] $EPR \leq -0.10$ – erosion, $-0.10 \leq EPR \leq +0.10$ – stability, $EPR \geq +0.10$ – accretion.
Explanation: *EPR* = end point rate.
Source: own study.

Fig. 4. Shoreline evolution between 2003 and 2010 carried out by the end point rate (*EPR*) statistical method along the coastline of Al-Hoceima Bay; B. = beach, M. = mouth; source: own study
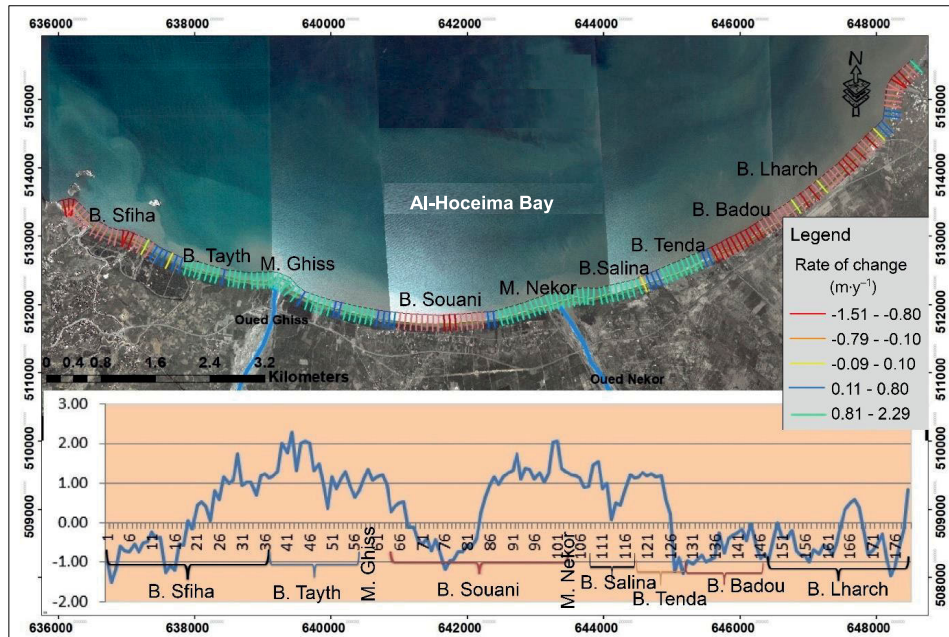
mobility index, shows spatial evolution along the coastline of this plain. Analysis of transects obtained using the DSAS model reveals the occurrence of both erosion and accretion zones along the sandy shores of the Al-Hoceima Bay coastline. Specifically, the western section of the Sfiha beach and the Lharch beach experienced erosion, with erosion rates of approximately −1.21 and −1.01 m·y^{-1}, respectively (Tab. 4). During this period, the shoreline position along this coastline advanced at the mouths of Ghiss and Nekôr. The Souani beach experienced a maximum erosion rate of approximately −1.51 m·y^{-1}. The Sfiha and Lharch

beaches retreated during this period. Fattening of this coastline was observed at the mouths of Ghiss and Nekôr. A maximum rate of accretion was observed at the mouth of Ghiss, reaching approximately +2.29 m·y^{-1} (transect 62). Sediment accumulation was observed not only on the left and the right banks of the two mouths but also on the Tayth beach. The increased deposition of sediment at the mouths of Ghiss and Nekôr can be attributed to heavy rainfall events in 2009 and 2010, which resulted in flooding in the plain.

Table 4. Assessment of beaches erosion and accretion in Al Hoceima Bay (2003–2010) using *EPR* index

Specification	Beach								
	Sfiha		Tayth	Souani			Salina	Badou	Lharch
Transect No.	3	27	42	63	76	103	108	129	174
Evolution evaluation	erosion	accretion	accretion	accretion	erosion	accretion	accretion	erosion	erosion
$EPR^{1)}$ (m·y^{-1})	−1.11	+1.30	+2.29	+1.50	−1.51	+2.10	+1.04	−1.12	−1.20

[1] $EPR \leq -0.10$ – erosion, $-0.10 \leq EPR \leq +0.10$ – stability, $EPR \geq +0.10$ – accretion.
Explanation: *EPR* = end point rate.
Source: own study.

The loosening of the MBK dam may have contributed to increased availability of sediment. As a result, these anthropogenic activities, combined with intense rainfall during the period, resulted in a higher sediment accumulation around the mouths of Ghiss and Nekôr. Coastal drift played a significant role in transporting this sediment toward the nearby beaches.

RATE CHANGE FROM 2010 TO 2020

During this 10-year period, the coastline of Al-Hoceima Bay underwent significant morphological changes (Fig. 5). The retreat of the coastline was observed at various beaches within the Ghiss–Nekôr plain, including Sfiha, Souani, Badou, and Lharch, each experiencing erosion rates that varied from one beach to another. In addition, the deltas of the Ghiss and Nekôr mouths experienced degradation during this period. The maximum erosion rate was observed at the western section of the Sfiha beach, with a rate of approximately -2.80 m·y^{-1} (transects 1–6) – Table 5. The mouth of Ghiss and the beaches of Souani, Badou, and Salina experienced shoreline retreat with an erosion rate of -1.49 m·y^{-1}. However, the shoreline advanced at the Tayth beach and the eastern section of the Lharch beach, with an accretion rate of about $+1.30$ m·y^{-1}. In addition, sediment accumulation was observed on the banks near the mouth of Ghiss. This degradation can be attributed to a decrease in sediment inputs from the Ghiss and Nekôr Rivers, which are the main sources of sediment supply to Al-Hoceima Bay. The decrease in sediment loading is primarily attributed to the construction of the MBK dam and the extraction of sand and aggregates from the Ghiss and Nekôr Rivers. These activities have reduced the natural supply of sediment to the coastal area. In addition, the shoreline position of the Sfiha beach has undergone significant changes, with approximately 13 m of sediment accumulation in the eastern part and regression in the western part of the beach. The degradation of the Sfiha beach can be attributed to the construction of tourism and development sites in 2018 and

2019, which have altered the natural dynamics of the beach. The beaches of Lharch and the eastern part of Sfiha have experienced significant shoreline advancement, with sediment accumulation extending over tens of meters. This sediment accumulation can be attributed to the gentle slope of these beaches and the sediment transport facilitated by coastal drift from the NE.

LONG-TERM CHANGE FROM 1964 TO 2020

The long-term changes in the shoreline of Al-Hoceima Bay from 1964 to 2020 were calculated and analysed (Figs. 6 and 7). This rate of change was calculated based on the statistical table obtained through the DSAS model, which was linked to the transect identifier using the ArcGIS tool. The erosion and accretion in this coastline, as measured by the *EPR* value, were classified into four categories: high erosion (less than -0.60 m·y^{-1}), low erosion (from -0.60 to -0.20 m·y^{-1}), and stable dynamic (from -0.20 to $+0.20$ m·y^{-1}), and low accretion (more than $+0.20$ m·y^{-1}). This analysis of shoreline classification for the coastal fringe of Al-Hoceima Bay over a period of 56 years (1964–2020) indicates that 69% of the coastline experienced erosion, 20% exhibited a stable dynamic, and 11% showed accretion. In general, the highest erosion rate, approximately -3.15 m·y^{-1}, was observed at the mouth of Nekôr, specifically at transect 114. However, the highest accretion rate of $+1.11$ m·y^{-1} was observed at the Sfiha beach, specifically at transect 20. The stable class of shoreline change was identified in the western sections of Sfiha and Lharch beaches. The accretion zone was located in the beaches of Badou, Quemado, and Sfiha. In addition, the beaches of Isli, Cala Bonita, and Souani experienced retreat of approximately -1.00 m·y^{-1}. The rocky beaches in the western part of Al-Hoceima Bay are characterised by their narrow width, typically ranging from 100 to 300 m in length and 5 to 40 m in width. This limited width makes them particularly vulnerable to coastal erosion. Due to their constrained size, these beaches are less effective at dissipating wave energy, leading to intensified erosion at the base of the carbonate cliffs and along the beach itself. This
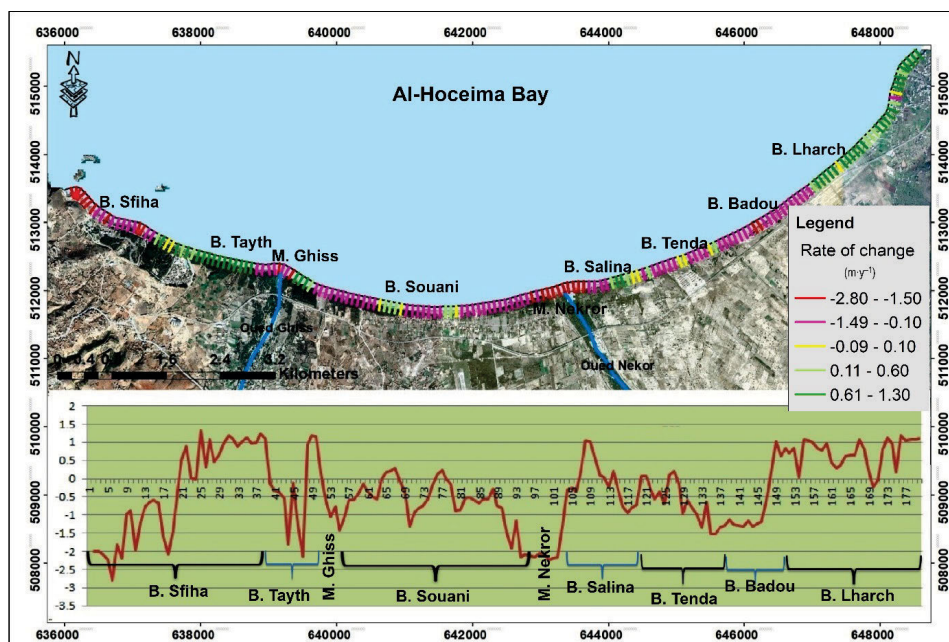

Fig. 5. Shoreline evolution between 2010 and 2020 carried out by the end point rate (*EPR*) statistical method along the coastline of Al-Hoceima Bay; B. = beach, M. = mouth; source: own study

Table 5. Assessment of beaches erosion and accretion in Al Hoceima Bay (2010–2020) using *EPR* index

Specification	Transect No.	Shoreline evolution – average (m)	Shoreline evolution – rate (m·y^{-1})
Sfiha	5	−28	−2.80
	25	+13	+1.30
Tayth	47	−14.90	−1.49
Ghiss mouth	54	−10	−1.00
Souani	90	−14.90	−1.49
Nekor mouth	101	−20	−2.00
Salina	108	+13	+1.30
Tenda	136	−15	−1.50
Badou	143	−11.20	−1.12
Lharch	167	+10.10	+1.01

1) $EPR \leq -0.10$ – erosion, $-0.10 \leq EPR \leq +0.10$ – stability, $EPR \geq +0.10$ – accretion.
Explanation: *EPR* = end point rate.
Source: own study.
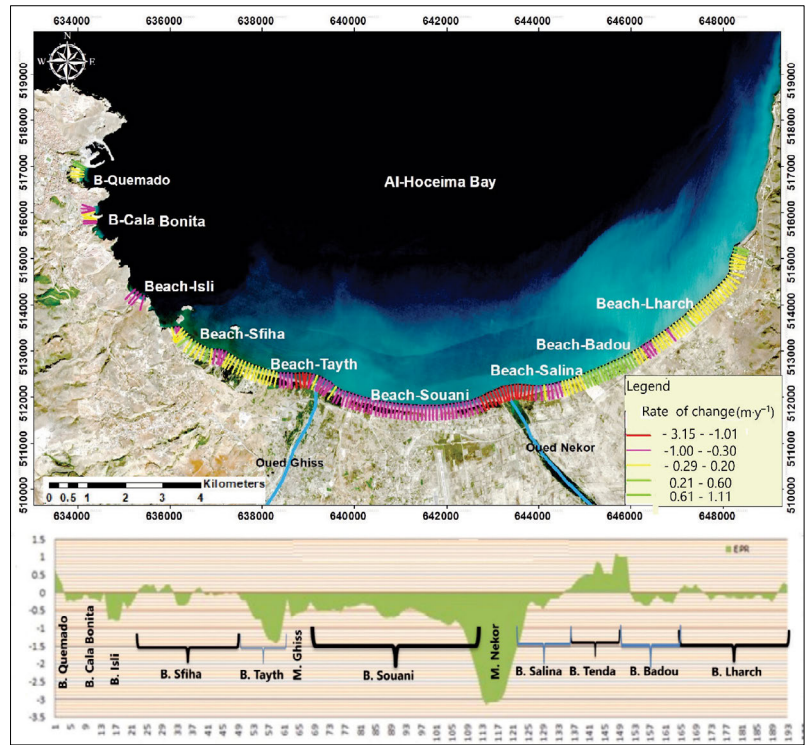
Fig. 6. Long-term evolution along the shoreline of Al-Hoceima Bay, between 1964 and 2020, analysed using the end point rate (*EPR*) statistical method; B. = beach, M. = mouth; source: own study
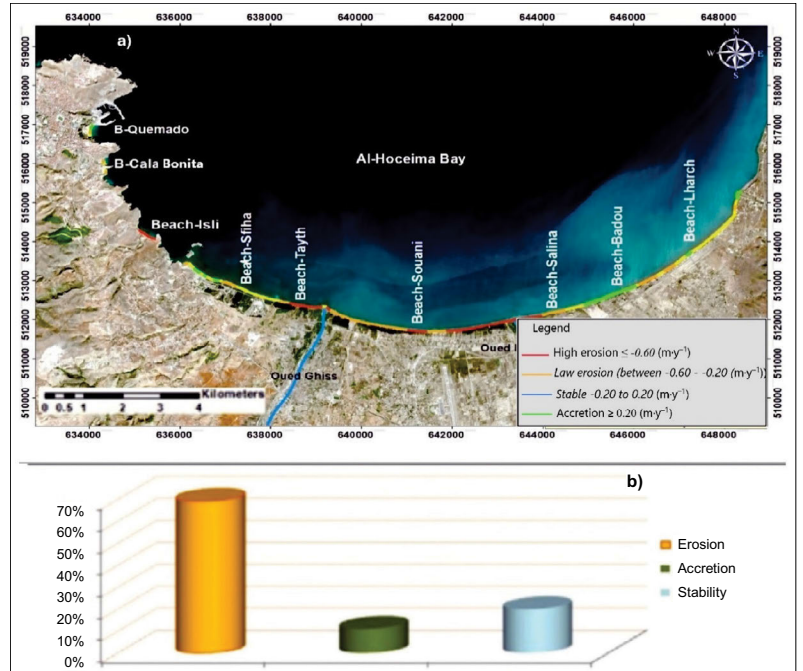
Fig. 7. Long-term (1964–2020) classification of the evolution of the shoreline of Al-Hoceima Bay: a) map, b) diagram represents the percentage of erosion, accretion, and stability; source: own study

process exacerbates cliff retreat and can result in significant land loss through landslides (Roberts and Williams, 2021; Giannakopoulos and Tsiropoulos, 2023). In general, during the period from 1964 to 2020 (Fig. 6), sediment accumulation was observed on the beaches of Sfiha, Quemado, and Badou, with a maximum accretion rate of +1.11 m·y^{-1}. However, many areas along this coastline were characterised by erosion, leading to shoreline retreat.

DISCUSSION

While studying the long-term shoreline change, numerous segments of the coast were found to be affected by erosion on various beaches. The maximum *EPR* values, as measured by the DSAS erosion and accretion model, were -3.15 m·y^{-1} for erosion and $+1.11$ m·y^{-1} for accretion. Several studies conducted in various areas have demonstrated changes in shoreline, which corroborate the current findings. Benkhattab *et al.* (2020), found coastal retreat of approximately 3.91 m·y^{-1} in the Tetouan region. Similarly, a retreat rate has been observed on the coasts of Saïdia (Bouabdallah and Larue, 2009), as well as on the Kenitra coast (Moussaid *et al.*, 2015) and Tahaddart coast (El Habti *et al.*, 2022). Retreat also affects the coasts of Egypt (Badr Hussein, Ibrahim and Mousa, 2023) and the Patras Gulf (Greece) (Depountis *et al.*, 2023), with rates varying from one region to another. Sandy beaches undergo spatiotemporal changes in their morphologies as a result of natural processes such as waves, tides, and river inputs (Bouabdallah and Larue, 2009; Moussaid *et al.*, 2015). Anthropogenic action, such as the construction of tourist and sand extraction sites, also contributes to these changes (Bouabdallah and Larue, 2009; Maiti and Bhattacharya, 2009; Moussaid *et al.*, 2015). The changes in the position of the shoreline have significantly impacted human activities, coastal infrastructure, and ecosystem services (Schlacher *et al.*, 2008).

Alterations to the coastline can significantly affect the ecosystem services offered by Al-Hoceima Bay in various ways. Specifically, coastal ecosystems like the sandy beaches along the bay, the dunes of Sfiha beach, and the vegetation cover play a crucial role in safeguarding the coast against erosion from waves and storms. As the coastline recedes, these natural ecosystems are often destroyed or disrupted, reducing their capacity to absorb wave energy and increasing the risk of flooding and the intrusion of seawater into the Ghiss–Nekôr aquifer. Moreover, the coastal ecosystems of this bay host a diverse range of marine and terrestrial species. Coastal changes can result in the loss of vital habitats for many species, including fish nurseries and breeding areas for seabirds, leading to a decline in species populations and a loss of biodiversity. In addition, Al-Hoceima Bay's coastline offers numerous recreational opportunities, such as swimming, fishing, tourism, and water-based activities. Coastal retreat can limit access to beaches and other recreational areas. Furthermore, the loss of natural beauty and the degradation of the coastal environment can reduce the attractiveness of these recreational destinations.

The historical analysis of shoreline changes along the coast of Al-Hoceima Bay from 1964 to 2020 revealed that approximately 69% of the rate of change in sandy coasts within Al-Hoceima Bay can be attributed to erosion. About 20% of the coastline remained stable, whereas 11% experienced accretion during the studied period (Figs. 6 and 7). The changes and degradation of the sandy beaches in Al-Hoceima Bay, particularly in the Ghiss–Nekôr plain, have been highly significant. Eroded river sediments from the watershed are deposited in the mouth of the Ghiss River, with a tendency for sediment deposition on the right bank. The Ghiss and Nekôr mouths act as reservoirs for significant amounts of detrital and soluble loads transported by coastal river basins (Lamgharbaj *et al.*, 2021). However, the Nekôr mouth experienced erosion during this period. The region is known for a gradual decrease in sediment flow because of

drought and the development of dams in the watershed of the two rivers, Ghiss and Nekôr, which supply this coastline. In general, several natural factors contribute to the acceleration of the rate of change along this coast. The Sfiha beach, for instance, is a relatively calm area protected from N–NE and S–SE swells by small cliffs on the left side and the presence of Nekôr islets. It forms a tombolo that experiences accretion rate of approximately $+1.11$ m·y^{-1}, primarily driven by the coastal drift of the NW–SE swells. The current generated by this swell facilitates the transportation of eroded sediments from the NE side to the SW side. In addition, NE swells cause coastal transit west of the bay.

This long-term result can be attributed to climate change in the Mediterranean, particularly the rise in the sea level. In Al-Hoceima Bay, shoreline changes are primarily driven by sea-level rise and shifts in storm patterns. The Alboran Sea, which includes this area, has seen a sea-level rise of about 2.5 to 3.0 mm·y^{-1}, slightly below the global average (Gomis *et al.*, 2008). This rise leads to increased coastal erosion and shoreline retreat, exacerbated by more frequent and intense storms (Hinkel *et al.*, 2014). Additionally, changes in wave climate affect sediment transport along the coast, further influencing the bay's shoreline dynamics (Vousdoukas *et al.*, 2020). The increase in sea-level rise will modify the stability and evolution of the coastal system (Paprotny and Terefenko, 2017). In the case of the Sfiha beach, the construction of numerous tourism complexes and the establishment of a promenade took place between 2018 and 2021. However, the development of infrastructure have resulted in damage and instability of the sand in the beach area. Furthermore, various actions and developments within the Ghiss–Nekôr watershed are likely to have affected the stability and natural evolution of the coastal zone. In general, the unprecedented urban expansion observed in the city of Al-Hoceima and the Ghiss–Nekôr plain, rapid reconstruction after the 2004 earthquake, and current growth in tourism significantly contributes to the proliferation of extraction sites. These sites aim to meet a high demand for construction materials. Material extraction along the beaches and in the valleys of the Ghiss and Nekôr rivers are detrimental to the stability of the bay's coastline. These extractions occur directly on the shore, on the upper parts of the beaches, within the dunes, and at the mouths of the Ghiss and Nekôr. One prominent factor is the construction of the MBK dam on the Nekôr River, which began in 1981. The MBK dam has significantly disrupted sediment dynamics in Al-Hoceima Bay by trapping sediment that would otherwise flow into the bay. This decrease in sediment supply has intensified shoreline erosion, as there is insufficient material to offset the effects of wave action. Additionally, coastal development and sand mining worsen these problems by increasing runoff and depleting sediment resources, respectively. Consequently, these factors create a complex interplay of erosion and accretion, disrupting the natural sediment balance along the shoreline of Al-Hoceima Bay.

The MBk and Ghiss dams, along with intensive land use and the impacts of climate change, could lead to significant environmental consequences. These include disruption of the sediment budget, exacerbation of coastal erosion, alteration of natural habitats, threats to both aquatic and terrestrial biodiversity, and an increased frequency of droughts, floods, and other extreme climate events. Another significant factor is the construction of the Jemaa dam on the Oued Ghiss, which began in 1991. These development of hydraulic facilities have sig-

nificantly reduced flow rates, and the amount of sediment transported downstream, thereby affecting the supply of sediments to the beaches in the bay. This decrease in inputs is responsible for the erosion of the most upstream part of the Nekôr delta. Furthermore, climate changes in recent decades have contributed to a decrease in flow, particularly at the Ghiss–Nekôr level. These combined climatic and anthropogenic impacts have intensified erosion and disrupted the sediment balance along the shoreline of Al-Hoceima Bay. The coastal frontline of the bay is subject to natural and anthropogenic pressures, such as sea-level rise because of climate change and tourism. The persistence of these pressures in the future could have catastrophic consequences for the bay's coastline. This reinforces the estimation of coastline retreat of approximately 94 m by 2,050 at the mouth of the Nekôr and 30 m at the Souani beach.

Concluding, it is crucial for local managers and decision-makers to incorporate management plans into territorial development projects to ensure the future of the sandy beaches in the region. These results also underline the necessity of implementing an effective strategy to counteract coastal erosion along this coastline. This involves several tangible actions, including the replenishment of sand on the heavily eroded beaches of Souani and Tayth. Implementing coastal regulations along the bay's beaches is of paramount importance. The aims are to prohibit the construction of structures near the coastline and reinforce environmental controls to limit detrimental activities such as construction or sand extraction from the beaches, as well as from the Ghiss and Nekôr Rivers. It is also recommended to construct sustainable tourist facilities on the beaches of Sfiha, Souani, and Lharch, which involve the use of environmentally friendly materials, coastal-friendly construction practices, the establishment of eco-responsible infrastructures, and the preservation of surrounding natural ecosystems. In addition, the dune systems of the Sfiha beach should be protected and restored using engineering techniques such as stabilisation through vegetation planting and installation of brushwood fencing. Finally, developing an urban planning scheme in compliance with coastal regulations, considering the most affected areas, and planning for the establishment of protected areas represent a comprehensive and essential approach for the preservation and restoration of sandy beaches in the region. It is equally crucial to actively involve local communities in the decision-making processes related to coastal management.

CONCLUSIONS

The study of historical changes in the shoreline of Al-Hoceima Bay is based on the interpretation of aerial photographs from 1964 until 2020. This study plays a crucial role in quantifying the rate of change affecting these areas. Over a span of 56 years, the position of the shoreline in this coastal zone has changed significantly, with approximately 69% erosion and 11% accretion observed. The coast of Al-Hoceima Bay exhibited alternating phases of shoreline retreat and progression, with a maximum retreat rate of −3.15 m·y^{-1} and an accretion rate of approximately +1.11 m·y^{-1} during the period from 1964 to 2020. This study revealed that the coast of Al-Hoceima Bay experienced significant erosion, particularly after 2003. The accelerated change in morphology is attributed to anthropogenic activities, specifically

the construction of tourist facilities at the Sfiha beach and sand extraction from the beaches and the Ghiss and Nekôr rivers. Furthermore, the construction of the MBK dam and climate change have led to a reduction in sediment availability, thereby affecting coastal dynamics. To enhance the understanding of sedimentary processes within the bay, ongoing approaches include the modelling of sediment dynamics. These studies aim to identify sedimentary cells and better understand factors that control the hydro-sedimentary function within the bay.

In light of the results of this study, it is crucial to implement integrated coastal management plans that incorporate nature-based solutions, such as the restoration of dunes and wetlands, to mitigate the impacts of the dams and climate change on the coastline of the Bay. Additionally, it is essential to develop a systematic monitoring programme to continuously track changes in coastal dynamics. This programme should enable real-time adjustments to management strategies based on collected data, while actively engaging local communities in conservation efforts and adaptation to coastal risks.

CONFLICT OF INTERESTS

All authors declare that they have no conflict of interests.

REFERENCES

Aangri, A. *et al.* (2022) "Predicting shoreline change for the Agadir and Taghazout coasts (Morocco)," *Journal of Coastal Research*, 38(5), pp. 937–950. Available at: https://doi.org/10.2112/JCOASTRES-D-22-00006.1.

Achalhi, M. *et al.* (2016) "The late Miocene Mediterranean-Atlantic connections through the North Rifian Corridor: New insights from the Boudinar and Arbaa Taourirt basins (northeastern Rif, Morocco)," *Palaeogeography, Palaeoclimatology, Palaeoecology*, 459, pp. 131–152. Available at: https://doi.org/10.1016/j.palaeo.2016.06.040.

Aouiche, I. *et al.* (2016) "Anthropogenic effects on shoreface and shoreline changes: Input from a multi-method analysis, Agadir Bay, Morocco," *Geomorphology*, 254, pp. 16–31. Available at: https://doi.org/10.1016/j.geomorph.2015.11.013.

Badr Hussein, K., Ibrahim, M. and Mousa, B.G. (2023) "Modeling and analysis of shoreline change in the Sidi Abdel Rahman coast area, Egypt," *NAŠE MORE: Znanstveni časopis za more i pomorstvo*, 70(1), pp. 23–37. Available at: https://doi.org/10.17818/NM/2023/1.4.

Barbier, E.B. *et al.* (2011) "The value of estuarine and coastal ecosystem services," *Ecological Monographs*, 81(2), pp. 169–193. Available at: https://doi.org/10.1890/10-1510.1.

Benaissa, C. *et al.* (2024) "GIS-based hydrochemical assessment of groundwater in the Bakoya Massif, Northern Morocco" *Desalination and Water Treatment*, 317, 100287. Available at: https://doi.org/10.1016/j.dwt.2024.100287.

Benkhattab, F.Z. *et al.* (2020) "Spatial–temporal analysis of the shoreline change rate using automatic computation and geospatial tools along the Tetouan coast in Morocco," *Natural Hazards*, 104(1), pp. 519–536. Available at: https://doi.org/10.1007/s11069-020-04179-2.

Bird, E.C.F. (1985) *Coastline changes: A global review*. Hoboken, NJ: Wiley.

Boak, E.H. and Turner, I.L. (2005) "Shoreline definition and detection: A review," *Journal of Coastal Research*, 21(4, 214), pp. 688–703. Available at: https://doi.org/10.2112/03-0071.1.

Bouabdallah, M. and Larue, J.P. (2009) "Évolution du littoral de la baie de Saïdia : Dynamique naturelle et impact des aménagements (Maroc oriental) [Evolution of the Saïdia Bay coastline: Natural dynamics and impact of developments (Eastern Morocco)]" *Physio-Géo. Géographie physique et environnement*, 3, pp. 113–130. Available at: https://doi.org/10.4000/physio-geo.878.

Boubkari, L. *et al.* (2022) "Neogene basins in Eastern Rif of Morocco and their potential to host native sulphur," *All Earth*, 34(1), pp. 90–106. Available at: https://doi.org/10.1080/27669645.2022.2097040.

Boye, C.B. *et al.* (2018) "Spatio-temporal analyses of shoreline change in the Western Region of Ghana," *Journal of Coastal Conservation*, 22(4), pp. 769–776. Available at: https://doi.org/10.1007/s11852-018-0607-z.

Carruthers, L. *et al.* (2023) "Coral reef island shoreline change and the dynamic response of the freshwater lens, Huvadhoo Atoll, Maldives," *Frontiers in Marine Science*, 10, pp. 1–18. Available at: https://doi.org/10.3389/fmars.2023.1070217.

Chen, C. *et al.* (2019) "The application of the tasseled cap transformation and feature knowledge for the extraction of coastline information from remote sensing images," *Advances in Space Research*, 64(9), pp. 1780–1791. Available at: https://doi.org/10.1016/j.asr.2019.07.032.

Crowell, M., Leatherman, S.P. and Buckley, M.K. (1991) "Historical shoreline change: Error analysis and mapping accuracy," *Journal of Coastal Research*, 7(3), pp. 839–852.

Depountis, N. *et al.* (2023) "Coastal erosion identification and monitoring in the Patras Gulf (Greece) using multi-discipline approaches," *Journal of Marine Science and Engineering*, 11(3), 654. Available at: https://doi.org/10.3390/jmse11030654.

El Habti, M.Y. *et al.* (2022) "Shoreline change analysis along the Tahaddart coast (NW Morocco): A remote sensing and statistics-based approach," *Journal of Coastal Research*, 38(6). Available at: https://doi.org/10.2112/JCOASTRES-D-22-00026.1.

El Mrini, A. *et al.* (2012) "An integrated approach to characterize the interaction between coastal morphodynamics, geomorphological setting and human interventions on the Mediterranean beaches of North-Western Morocco," *Applied Geography*, 35(1–2), pp. 334–344. Available at: https://doi.org/10.1016/j.apgeog.2012.08.009.

El-Khantoury, I., Obda, K. and Achiban, H. (2020) "Wavelet analysis: A link between the North Atlantic Oscillation and winter drought in the Mediterranean watersheds of the Western Rif (North Morocco)," *European Scientific Journal, ESJ*, 16(15), 99. Available at: https://doi.org/10.19044/esj.2020.v16n15p99.

Fenster, M. and Dolan, R. (1994) "Large-scale reversals in shoreline trends along the U.S. mid-Atlantic coast," *Geology*, 22(6), pp. 543–546. Available at: https://doi.org/10.1130/0091-7613(1994)022<0543:LSRIST>2.3.CO;2.

Fletcher, C.H. *et al.* (2012) *National assessment of shoreline change: Historical shoreline change in the Hawaiian Islands. Open-File Report 2011–1051*. Reston, Virginia: U.S. Geological Survey. Available at: https://doi.org/10.3133/ofr20111051.

Ford, M. (2011) "Shoreline changes on an urban atoll in the Central Pacific Ocean: Majuro Atoll, Marshall Islands," *Journal of Coastal Research*, 28(1), pp. 11–22. Available at: https://doi.org/10.2112/JCOASTRES-D-11-00008.1.

Giannakopoulos, C. and Tsiropoulos, Z. (2023) "Coastal erosion and cliff stability: Case studies from the Mediterranean," *Journal of Coastal Research*, 39(2), pp. 356–367.

Gomis, D. *et al.* (2008) "Low frequency Mediterranean Sea level variability: The contribution of atmospheric pressure and wind," *Global and Planetary Change*, 63(2–3), pp. 215–229. Available at: https://doi.org/10.1016/j.gloplacha.2008.06.005.

Hakkou, M. *et al.* (2018) "Multi-decadal assessment of shoreline changes using geospatial tools and automatic computation in Kenitra coast, Morocco," *Ocean & Coastal Management*, 163, pp. 232–239. Available at: https://doi.org/10.1016/j.ocecoaman.2018.07.003.

Himes-Cornell, A., Grose, S.O. and Pendleton, L. (2018) "Mangrove ecosystem service values and methodological approaches to valuation: Where do we stand?" *Frontiers in Marine Science*, 5, 376. Available at: https://doi.org/10.3389/fmars.2018.00376.

Hinkel, J. *et al.* (2014) "Coastal flood damage and adaptation costs under 21st-century sea-level rise," *Proceedings of the National Academy of Sciences*, 111(9), pp. 3292–3297. Available at: https://doi.org/10.1073/pnas.1222469111.

Hossain, S.A. *et al.* (2022) "Coastal vulnerability assessment of India's Purba Medinipur-Balasore coastal stretch: A comparative study using empirical models," *International Journal of Disaster Risk Reduction*, 77, 103065. Available at: https://doi.org/10.1016/j.ijdrr.2022.103065.

Jaykumar, K. and Malarvannan, S. (2016) "Assessment of shoreline changes over the Northern Tamil Nadu Coast, South India using WebGIS techniques," *Journal of Coastal Conservation*, 20(6), pp. 477–487. Available at: https://doi.org/10.1007/s11852-016-0461-9.

Kumar Das, S. *et al.* (2021) "Shoreline change behavior study of Jambudwip island of Indian Sundarban using DSAS model," *The Egyptian Journal of Remote Sensing and Space Science*, 24(3, Part 2), pp. 961–970. Available at: https://doi.org/10.1016/j.ejrs.2021.09.004.

Lamgharbaj, M. *et al.* (2021) "Geochemical and mineralogical characterization of coastal sediments in Al-Hoceima Bay (Central Rif, Morocco)," *E3S Web of Conferences*, 298, 04003. Available at: https://doi.org/10.1051/e3sconf/202129804003.

Lanfelder, L.J., Stafford, D.B. and Amein, M. (1970) "Coastal erosion in North Carolina," *Journal of the Waterways, Harbors and Coastal Engineering Division*, 96(2), pp. 531–545. Available at: https://doi.org/10.1061/AWHCAR.0000032.

Luijedijk, A. *et al.* (2018) "The state of the world's beaches," *Scientific Reports*, 8(1), 6641. Available at: https://doi.org/10.1038/s41598-018-24630-6.

Mageswaran, T. *et al.* (2021) "Impact of sea level rise and shoreline changes in the tropical island ecosystem of Andaman and Nicobar region, India," *Natural Hazards*, 109(2), pp. 1717–1741. Available at: https://doi.org/10.1007/s11069-021-04895-3.

Maiti, S. and Bhattacharya, A.K. (2009) "Shoreline change analysis and its application to prediction: A remote sensing and statistics based approach," *Marine Geology*, 257(1), pp. 11–23. Available at: https://doi.org/10.1016/j.margeo.2008.10.006.

Martinez, C. *et al.* (2022) "Coastal erosion in sandy beaches along a tectonically active coast: The Chile study case," *Progress in Physical Geography: Earth and Environment*, 46(2), pp. 250–271. Available at: https://doi.org/10.1177/03091333211057194.

Moussaid, J. *et al.* (2015) "Using automatic computation to analyze the rate of shoreline change on the Kenitra coast, Morocco," *Ocean Engineering*, 71, pp. 71–77. Available at: https://doi.org/10.1016/j.oceaneng.2015.04.044.

Muskananfola, M.R., Supriharyono and Febrianto, S. (2020) "Spatio-temporal analysis of shoreline change along the coast of Sayung Demak, Indonesia using Digital Shoreline Analysis System,"

Regional Studies in Marine Science, 34, 101060. Available at: https://doi.org/10.1016/j.rsma.2020.101060.

Nouayti, N. *et al.* (2022) "Determination of physicochemical water quality of the Ghis-Nekor aquifer (Al Hoceima, Morocco) using hydrochemistry, multiple isotopic tracers, and the geographical information system (GIS)," *Water*, 14(4), 606. Available at: https://doi.org/10.3390/w14040606.

Pajak, M.J. and Leatherman, S. (2002) "The high water line as shoreline indicator," *Journal of Coastal Research*, 18(2), pp. 329–337. Available at: https://journals.flvc.org/jcr/article/view/81276/78416 (Accessed: May 06, 2023).

Paprotny, D. and Terefenko, P. (2017) "New estimates of potential impacts of sea level rise and coastal floods in Poland," *Natural Hazards*, 85(2), pp. 1249–1277. Available at: https://doi.org/10.1007/s11069-016-2619-z.

Roberts, M. and Williams, T. (2021) "Shoreline response to sea-level rise and erosion trends: A comparative analysis," *Journal of Coastal Research*, 37(4), pp. 902–919.

Salim, F.Z. *et al.* (2021) "A diachronic study of the Mediterranean coastline: A geometric approach," *E3S Web of Conferences*, 234, 00039. Available at: https://doi.org/10.1051/e3sconf/202123400039.

Santos, C.A.G. *et al.* (2021) "Analysis of long- and short-term shoreline change dynamics: A study case of João Pessoa city in Brazil," *Science of The Total Environment*, 769, 144889. Available at: https://doi.org/10.1016/j.scitotenv.2020.144889.

Schlacher, T.A. *et al.* (2008) "Sandy beach ecosystems: key features, sampling issues, management challenges and climate change impacts," *Marine Ecology*, 29(s1), pp. 70–90. Available at: https://doi.org/10.1111/j.1439-0485.2007.00204.x.

Sheik, M. and Chandrasekar (2011) "A shoreline change analysis along the coast between Kanyakumari and Tuticorin, India, using Digital Shoreline Analysis System," *Geo-Spatial Information Science*, 14(4), pp. 282–293. Available at: https://doi.org/10.1007/s11806-011-0551-7.

Shin, B. and Kim, K. (2015) "Estimation of shoreline change using high resolution images," *Procedia Engineering*, 116, pp. 994–1001. Available at: https://doi.org/10.1016/j.proeng.2015.08.391.

Syvitski, J.P.M. *et al.* (2005) "Impact of humans on the flux of terrestrial sediment to the global coastal ocean," *Science*, 308(5720), pp. 376–380. Available at: https://doi.org/10.1126/science.1109454.

Taher, M. *et al.* (2022) "The risk mapping of coastal flooding areas due to tsunami wave run-up using DAS model and its impact on Nekor Bay (Morocco)," *Ecological Engineering & Environmental Technology*, 23(4), pp. 136–148. Available at: https://doi.org/10.12912/27197050/150310.

Thieler, E.R. *et al.* (2009) *The Digital Shoreline Analysis System (DSAS) Version 4.0 – An ArcGIS extension for calculating shoreline change (No. 2008–1278). Open-File Report*. Reston, Virginia: U.S. Geological Survey. U.S. Geological Survey. Available at: https://doi.org/10.3133/ofr20081278.

Vousdoukas, M.I. *et al.* (2020) "Sandy coastlines under threat of erosion," *Nature Climate Change*, 10, pp. 260–263. Available at: https://doi.org/10.1038/s41558-020-0697-0.